RSC Advances

ROYAL SOCIETY OF CHEMISTRY

www.rsc.org/advances

Comparison of transport between two bacteria in saturated porous media with distinct pore size distribution

Hongjuan Bai *, Nelly Cochet, Audrey Drelich, André Pauss, Edvina Lamy

Sorbonne universités, Université de technologie de Compiègne, ESCOM, EA 4297 TIMR, Centre de recherche Royallieu - CS 60 319 - 60 203 Compiègne cedex, France

*Corresponding author. Tel.: +33 344237933.

E-mail address: hongjuan.bai@utc.fr (H.J. Bai)

Abstract

The transport of *Escherichia coli* (1.1 μm) and *Klebsiella* sp. (1.5 μm) were performed in three porous media with different grain and pore size distributions under saturated flow conditions to explore the coupled effect of porous size distribution and bacteria cell properties on microbial transport. A two-region mobile-immobile model that account for non-uniform transport in porous media was used to quantify the uniformity of bacteria flow pathways. Bacteria flow pathways were more non-uniform compared to those of water tracer for each porous medium. While the non-uniformity of bacteria flow pathways increased with the increasing of the physical heterogeneity of the porous media for *Klebsiella* sp., no clear tendency was obtained for *E. coli*. Different behaviors in term of *E. coli* and *Klebsiella* sp. cells retention were observed: similar retention rates were obtained in all porous media for the motile *E. coli*, whereas the non-motile *Klebsiella* sp. retention decreased in the medium that exhibited larger pores and a wide range of the pore size distribution. These results indicated that bacteria transport and retention were simultaneously dependent to both pore size distribution and bacteria cell properties.

Keyword: bacteria transport; pore size distribution; cell properties

1. Introduction

It has been reported that microorganisms such as bacteria, protozoan parasites and viruses that come from human or animal wastes can travel through soil to groundwater from a contamination source,[1, 2] and if these microorganisms are present in drinking water, they can result in serious health hazards.[3-5] In addition, they cannot

only travel attached to abiotic particles, but also facilitate the transport of a variety of metals and other chemicals.[6-9] Thus, a better understanding of the transport and retention of microorganisms in porous media is necessary to protect the surface and groundwater supplies from contamination and to assess the risk from microorganisms in groundwater.[10, 11] On the other hand, the investigation of the transport and retention of bacteria in porous media has also a great practical importance in other environmental applications, such as in-situ soil bioremediation project and riverbank filtration.[3, 12, 13]

It has widely been reported in the existing literature that bacteria transport is highly influenced by grain or pore size of the porous media. Thus many previous studies have been focused on bacteria transport in homogeneous porous media,[14-16] and several publications are also available on the bacteria transport in heterogeneous porous media with different pore size geometry.[17, 18] *Escherichia coli* is the most commonly used bacteria for evaluating bacteria transport in porous media. This bacterium has been used to investigate the factors that control microbial transport in porous media. These factors include bacteria concentration,[19] medium characteristics such as grain size,[1] the presence of surface coatings,[20] matrix structure,[21] hydrodynamics properties such as pore water velocity[19, 22-25] and water content,[26] and chemical factors such as pH and ionic strength.[27-31] To understand the role of the porous grain size on bacteria transport, porous media with different grain sizes have been employed in literature studies. A porous medium constituted by grains with different sizes implies different pore sizes accessible for bacteria transport. Recent publications have demonstrated that not only pores sizes but also their distribution can strongly affect the transport and retention of colloidal particles in porous media under various conditions.[32-35] While the pore size effect has been extensively studied, one drawback associated with the current body of literature is the limited number of studies examining the pore size distribution of the porous media and its effect on bacteria transport and retention.[17] Thus, preferential transport of bacteria through macropores has been observed in heterogeneous porous media with simple geometry, constituted by the macropore insertion into homogenous matrix sand.[25, 36] Other research work has been carried out in real soils with a complicated geometry of macropores.[17, 37] However the difficulties associated to the control of the hydrodynamic conditions as well the difficulty to obtain an accurate description of

macropores geometry makes it hard to reach conclusive results concerning bacteria transport in these complicated real porous systems. The transport of model colloid particles (latex microspheres) under laboratory conditions in porous media composed by mixing sands with different grain size have been studied by Leij and Bradford.[38] These authors concluded that the relatively small sample size and the complex flow pattern in the composite medium made difficult to reach definitive conclusions regarding transport parameters for colloid transport. Besides, bacteria transport studies in aggregate media with micro- and macroporosity are very limited in the current literature. In such complex systems, solute migration is mainly controlled by inter-aggregate pores (macropores/mobile phase) in which dispersion and advection occurs and solute diffusion take place from inter-aggregate openings to intra-aggregate pores (micropores).[39, 40, 41] However the existing studies in aggregate media are only limited to solute transport processes. To the best of our knowledge, there is no study on the bacteria transport and retention in aggregate porous media. Such reports underlined the need for more studies evaluating the effect of pore size distribution of porous media on bacteria transport and retention.

The factors affecting bacteria transport including cell characteristics like cell types and motility,[42-44] hydrophobicity,[45] cell size and shape,[46] population growth[44] have also been extensively studied. However, their role on bacteria transport has been mainly investigated in homogenous sandy media. And the role on bacteria transport through heterogeneous porous media has received considerably less attention.

The aim of this study was to investigate the coupled effect of bacteria cell characteristics and physical characteristic of the porous media on the microbial transport. Miscible transport experiments were performed in three porous media with different grain and pore size distributions under saturated steady state flow conditions. Two different representative cell types, *Escherichia coli* and *Klebsiella* sp. were used as biotic colloids for transport experiments. Breakthrough curves of bacteria were measured and numerically simulated using a two-region mobile-immobile model,[47] which account for non-uniform transport in heterogeneous porous media. Mass balance calculations and the final retained bacteria in the column after transport experiments, deduced from experimental observations, as well fitted model transport parameters were to compare the transport of two bacteria.

2. Materials and methods

2.1. Porous media characterization and electrolyte solutions

Three different porous media were employed for column experiments in this study: (a) a homogenous Fontainebleau sand (F) which had a particle size distribution of 0.25-0.54 mm, with a median grain size (d_{50}) of 0.36 mm, (b) a heterogeneous Compiègne sand (C) which had a particle size distribution of 0.58-1.48 mm, with a median grain size (d_{50}) of 0.90 mm, and (c) a heterogeneous calcareous gravel (G) which had a particle size distribution of 0.4-5.0 mm, with a median grain size (d_{50}) of 1.5 mm. The gravel had a dual porosity: intra-granular porosity inside particles and inter-granular porosity between particles. Lamy et al. performed water absorption experiments for the same gravel and they reported that matrix intra-porosity correspond to about 50% of the total porosity (78.5% ± 0.5%)[47]. Prior to each experiment, all porous media were washed and rinsed thoroughly with deionized water to eliminate the fine particles, dried in an oven at 105 ^{o}C, and then sterilised in the autoclave at 121^{o}C for 30 minutes. Finally, they were stored in screw cap sterile beakers for further use in column transport experiments. The pore size distribution for all porous media was measured by Mercury Intrusion Porosimetry technique (Micromeritics, AutoPore IV 9500 V1.07).

The zeta potential of each porous medium, measured by a Zetasizer (3000 HAS, Malvern Instruments Ltd, UK), reached –39.6 ± 1.8 mV for Fontainebleau sand, –20.5 ± 1.8 mV for Compiègne sand, and –12.5 ± 1.8 mV for the gravel.

The background electrolyte solution for the bacterial characterization and transport experiments consisted of 0.1 mmol/L NaCl solution (pH = 5.89). To characterize the hydrodynamic properties of the porous media, 0.01 mol/L KBr solution (for both Fontainebleau and Compiègne sand) and 0.05 mol/L NaCl solution (for the gravel) were used as a conservative tracer.

2.2 Preparation and characterization of bacteria suspension

2.2.1 Bacteria preparation

The bacterial strains employed in this work were *Escherichia coli* (ATCC 25255) and *Klebsiella* sp. (*Klebsiella oxytoca*). *Escherichia coli,* a commonly used indicator of fecal contamination,[46, 48] is a gram-negative, motile, rod-shaped bacterium. *Klebsiella* sp. is a gram-negative, non-motile bacterial strain, which is ubiquitous in nature, and its nonclinical habitats encompass not only the gastrointestinal tract of

mammals but also environmental sources such as surface water, soil and plants.[49-51] Both bacterial strains were grown on DEV nutrient agar plates consisting of peptone from meat (10.0 g), meat extract (10.0 g), sodium chloride (5.0 g), agar (18.0 g) and distilled water (1000 mL). For column transport experiments, both bacterial strains were cultivated at 30 ^{o}C in the nutrient broth (ISO, APHA) under continuous agitation at 160 rpm by a thermo stated shaker (CH-4103, Bottmingen). The nutrient broth consisted of peptone (5.0 g), meat extract (3.0 g), and distilled water (1000 mL).

The bacterial cells were harvested from the nutrient broth in their early stationary phase (6 h for *E. coli* and 7 h for *Klebsiella* sp.) by centrifugation (Eppendorf, Centrifuge 5810R) (4000 rpm, 10 min, 4 ^{o}C). Then they were washed twice with a 0.1 mmol/L NaCl (Fisher Scientific) solution (pH = 5.89) and re-suspended in an identical NaCl solution. The same 0.1 mmol/L NaCl solution was also used as the background electrolyte solution for the transport experiments.

Each bacteria suspension with a known concentration was prepared with distilled water, adjusted with 0.1 mmol/L NaCl solution in this study. This step allows providing a good estimation of the total bacteria mass balance, partitioned between the effluent and soil particles. The actual bacterial concentrations in the influent solution were determined using the method of bacteria enumeration on the nutrient agar plates after incubation at 37^{o}C overnight[52] to monitor for exudates formation and possible cell aggregation. The optical density of the bacterial suspension was measured before and after the experiments. No changes in the optical density was observed, which indicated that the bacterial suspension remained stable over the duration of each transport experiment.[53]

2.2.2. Cell properties: cell size distribution, electrophoretic mobility and hydrophobicity

Several studies have reported that cell size and shape may greatly influence colloidal transport and retention in granular porous media.[54, 55] However, the cell size distribution of bacteria can also be a key factor in prediction of transport behavior [56]. The size distribution (equivalent spherical diameter) of *E. coli* and *Klebsiella* sp. were measured using a Zetasizer 3000 HAS (Malvern Instruments Ltd, UK).

The zeta potential which governs colloid stability[56] was measured by dynamic light scattering (Zetasizer 3000 HAS, Malvern Instruments Ltd, UK) for both bacteria

at ionic strength of 0.1 mmol/L NaCl. The measurements were conducted in triplicates for each cell suspension. The zeta potential values of the cells and porous media permitted the determination of DLVO interaction parameters and interaction energy profiles, which were calculated using the approach presented by Redman et al.[57] The Hamaker constant was set to 6.5×10^{-21} J for bacteria.[57]

The hydrophobicity adhesion to hydrocarbon (MATH) approach was used to determine the hydrophobicity of both bacterial strains.[58, 59] The test was performed under the following conditions: the bacteria were harvested at early stationary phase by centrifugation and the bacteria were washed twice with phosphate buffer (pH = 7.2) and the total cell number was determined by counting on agar plates. Then 3 mL of bacteria suspension was mixed with 0.3 mL of hexadecane (Fisher Scientific) and the mixture was vortexed during 2 minutes. After the phases were clearly separated, counting was performed on DEV agar plates containing the sample from the aqueous phase. The fraction partitioned to the hydrocarbon phase was calculated from the difference between the total cell number and the remaining cell number of the aqueous phase. The analysis was performed in triplicate for each sample.

2.3 Batch experiments

Batch experiments were performed on 150 mL conical flasks, each flask containing 5 g of porous media and 25 mL of a known initial concentration of bacteria suspension. Each conical flask was agitated on an orbital shaker to equilibrate at 160 rpm, at 25^{o}C for 1 hour. The duration of 1 hour equilibrium period was used here to be consistent with the time duration of column transport procedures. The initial and final concentrations of bacteria in the suspension were determined by using the spread plate methods. A blank experiment (no sand) was also run to quantify the potential for bacteria growth or death in the 0.1 mmol/L NaCl solution at 25 ^{o}C.

2.4 Column transport experiments

A Plexiglas column with an inner diameter of 3.3 cm and a height of 17.0 cm was employed for the transport experiments. Prior to each experiment, all column components, solutions and materials were sterilized. The pump, tubing and other column components that could not withstand autoclaving were sterilized with 96% ethyl alcohol (Fisher Scientific). All the transport experiments were performed in the Biological Safety Cabinet (Thermo Scientific, NFX44-201). Small quantities of each

porous medium were successively introduced into each column after being homogenously packed, to achieve homogenous distribution of the porous media into the columns. The total porosities of the porous media were calculated from their bulk densities. The later was estimated after packing the columns. The average total porosity of the porous beds were 0.34 ± 0.01, for Fontainebleau sand 0.44 ± 0.01 for Compiègne sand and 0.78 ± 0.01, for the gravel. The mean total pore volume (V_0), obtained by weighting each column before and after water saturation reached 58.8 ± 1.2 cm^3 for Fontainebleau sand, 68.2 ± 3.0 cm^3 for Compiègne sand and 100.9 ± 1.0 cm^3 for the gravel.

Prior to each experiment, the column was flushed upward under saturated conditions with about 3 pore volumes of the background electrolyte solution at a steady Darcy velocity of 0.42 ± 0.01 cm/min using a peristaltic pump (ISMATEC, IDEX corporation). Then the flow was reversed and the column was rinsed with about 10 pore volumes before starting the transport experiments. The solution chemistry conditions were verified by determining both conductivity and pH of the effluent solutions.

A short pulse of tracer solution (20 mL) was injected into each column experiment, followed by 0.1 mmol/L NaCl washing solution to background levels. The effluent conductivity was continuously measured to follow the tracer breakthrough using a conductivity meter (SevenMulti, METTLER TOLEDO) and then converted to tracer concentration. The pore water volume for each experiment, measured be weighting the column before and after transport experiment, remained the same. This indicated no change in the total porosity of the porous media, indicating no porous media property alteration.

For bacteria transport experiments, a 20 mL pulse of bacterial suspension ($\approx 10^8$ CFU/mL) was injected into each column experiment followed by the background electrolyte solution at the same flow rate as for the tracer experiments. The optical density at 600 nm was continuously measured at the column outlet by using a spectrophotometer (Perkin Elmer, Lambda 25). The absorbance bacteria breakthrough was then converted to concentration in order to monitor bacteria breakthrough curves (BTC). The total number of retained bacteria was determined for all columns after transport experiments. In this case, the saturated porous medium was carefully excavated in 9 layers and placed into 9 vials containing excess sterile 0.1 mmol/L of

NaCl solution. Then the vials were slowly shaken for 15 minutes to liberate any reversibly retained bacteria. Finally, the bacterial concentrations in the excess solution were determined by plate counting. Water and porous media filled vials were placed in an oven (110 ^{o}C) overnight to volatilize the remaining solution from porous media. The volume of water and the mass of the dry porous media in each vial was determined from mass balance by measuring the weight of empty vials, water and porous media filled vials, and porous media filled vials. The overall bacteria mass recovery (M_{total}) was subsequently determined as the sum of the amount of bacteria recovered in the effluent (M_{eff}) and the amount of bacteria retained in the porous medium ($M_{retained}$). All experiments were conducted in triplicate. The experimental set-up used for transport experiments is shown in Fig.1 and the overview of experimental conditions is shown in Table 1.

2.5 Breakthrough curves analysis

Tracer and bacterial breakthrough curves (BTCs) were plotted by the effluent concentration of tracer and bacteria. Mass balance (MB) and retardation factor (R) were estimated by the zero- and first- order moments of the BTCs:[60]

$$\mu_0 = \int_0^{+\infty} \frac{C(\mathrm{t})}{C_0}\mathrm{d}t\ ,\quad \mu_1 = \int_0^{+\infty} \mathrm{t}\frac{C(\mathrm{t})}{C_0}\mathrm{d}t \tag{1}$$

where μ_0 and μ_1 are the zero- and first- order moments of the elution curve, respectively; C(t) and C_0 are the time-dependent and initial concentration of the solute and bacteria. Mass balance (MB) corresponds to the ratio of the tracer or colloids mass recovered at the column outlet to their mass injected at the column inlet, and it was given by the following expression:[47]

$$MB = \frac{\mu_0}{\delta_{\mathrm{t}}} \tag{2}$$

where δt is the duration time of the injection for the tracer or bacteria into the column (min). Retardation factor was estimated by the ratio of residence time (t_s) for the tracer or bacteria to the theoretical water resident time (τ_s), and the mean tracer or bacteria resident time and theoretical water resident time can be calculated by the following equations:[47]

$$t_s = \frac{\mu_1}{\mu_0} - \frac{\delta_t}{2}, \quad \tau_s = \frac{L \cdot \theta}{q} \tag{3}$$

where L is the length of the column (cm), θ is the total volumic water content of the column and q is Darcy velocity (cm/min).

2.6 Mathematical modeling

In this work, tracer and bacteria transport experiments were simulated by HYDRUS-1D to predict transport parameters on the basis of the two-region mobile-immobile water (MIM) model.[61]

The governing equations of MIM model used in this study are written as:[61, 62]

$$\theta_m \frac{\partial C_m}{\partial t} + \theta_{im} \frac{\partial C_{im}}{\partial t} + \rho \frac{\partial s}{\partial t} = \theta_m D_m \frac{\partial^2 C_m}{\partial x^2} - q \frac{\partial C_m}{\partial x} \tag{4}$$

$$\theta_{im} \frac{\partial C_{im}}{\partial t} = \alpha (C_m - C_{im}) \tag{5}$$

$$\rho \frac{\partial s}{\partial t} = \theta_m k_{att} C - k_d \rho s \tag{6}$$

where θ_m and θ_{im} are the volumetric water contents in both mobile and immobile regions (cm^3/cm^3); C_m and C_{im} are the relative concentrations of mobile and immobile regions (mol/L or N_c/cm^3, N_c denotes the counts of bacteria), respectively; D_m is the dispersion coefficient of the mobile region (cm^2/min); q is the Darcy velocity (cm/min) defined as: $q = Q/S$ with the total flow Q and the column section S and α is the solute exchange rate between the two regions. The pore water velocity (υ_m) of the mobile region can be estimated as following: $\upsilon_m = q/\theta_m$. ρ is the bulk density of the porous media (g/cm^3); s is the bacterial concentrations in solid phase (N_c/g) and other variables were defined earlier. k_{att} is the bacterial attachment coefficient (1/min) and k_d is the first-order detachment coefficient (1/min). For tracer simulation, the term $\rho \frac{\partial s}{\partial t} = 0$.

Due to the limited pore volume of bacteria injection into the columns we assumed that bacteria retention to the porous media was an irreversible process. Thus the detachment coefficients were neglected in this work.

The MIM model was fitted to the experimental BTCs with the proper initial

conditions and boundary for the column transport experiments by the HYDRUS-1D code. The code allowed us to fit simultaneously the parameters of λ, α and θ_m (via θ_{im}) for tracer data, and the parameters λ, α, θ_m (via θ_{im}) and k_{att} for bacteria data using the inverse solution. The dispersivity of the medium λ (cm) which was assumed to be an intrinsic characteristic can be determined as follows:[47] $\lambda = (D_m \cdot \theta_m)/q$. The mobile water fraction (θ_m/θ) was estimated for each transport experiment to characterize the flow uniformity, were $\theta_m = \theta - \theta_{im}$ (θ is the total water content).

3. Results and discussion

3.1 Characterization of granular porous media

3.1.1 Pore size distribution

As shown in Fig. 2, the Fontainebleau sand revealed a median pore diameter, d_p, around 55 μm with a pore size distribution ranged from 5 to 200 μm. The median d_p for Compiègne sand was around 108 μm with a pore size distribution, ranging from 5 to 300 μm. The dual porosity gravel revealed a wide range of pore size distribution: one mode made of by small pores, with pore size diameter ranging from 0.005 to 5 μm with a peak obtained at 0.035 μm, and a second one with larger pores. The second mode, ranging from 5 to 360 μm, presented a two peaks shape pore size distribution: a first peak obtained at 15 μm and a second one at 200 μm.

3.2 Characterization of bacteria

3.2.1 Cell properties: cell size distribution, electrophoretic mobility and hydrophobicity

The cell size distribution (equivalent spherical diameter) for both *E. coli* and *Klebsiella* sp., suspension at an ionic strength of 0.1 mmol/L are presented in Fig. 3. The equivalent spherical diameter for *E. coli* ranged from 0.98 to 1.30 μm with a median cell size around 1.11 μm. *Klebsiella* sp. revealed an equivalent spherical diameter, ranging from 1.35 to 1.80 μm with a median cell size of 1.58 μm. Both bacteria presented similar zeta potential values (–41.1 ± 0.65 mV for *E. coli* and –33.2 ± 0.29 mV for *Klebsiella* sp.). MATH test results suggested that about 43.6% ± 3.7% of the cells were partitioned into the hydrocarbon for *E. coli*, suggesting a higher hydrophobicity of this strain comparing to *Klebsiella* sp. with 27.9% ± 3.1% of the

cells partitioned into the hydrocarbon.

3.3 Electrokinetic characterization

The DLVO calculations (Table 2) and interaction energy profiles (Fig. 4) showed the existence of substantial repulsive energy barriers for all bacteria-porous media systems, which limit the interactions between bacteria and porous media. However, because of a variable depth of a secondary minimum of energy, bacteria may still interact with the porous media by retention (Table 2). Because a thermal energy of a bacterium is on the order of 0.5 kT,[63, 64] the secondary minima depths shown in Table 2 close to or higher than 0.5 kT should be sufficient to retain bacteria cells in the porous media.

3.4 Batch experiments

Batch experiments suggested that under unfavorable attachment conditions (25 ^{o}C, pH = 5.89, Ionic strength = 0.1 mmol/L, negatively charged bacteria and negatively charged porous media), the initial and final concentrations of *E. coli* and *Klebsiella* sp. were almost identical (data not shown). Blank batch experiments suggested that bacteria growth or death during the experiment were not significant.

3.5 Transport experiments

3.5.1 Water flow in porous media with distinct pore size distribution

Experimental and simulated tracer breakthrough curves obtained for all porous media are plotted in Fig. 5a. Experimental tracer BTCs obtained for Fontainebleau sandy columns presented a symmetrical shape that indicate a uniform flow in this medium. The BTCs obtained for both Compiègne sandy and gravel columns were more asymmetrical in shape, with an early breakthrough and a substantial tailing, compared to Fontainebleau sandy columns. The peak of these elution curves occurred before $1 V/V_0$. All these information are indicative of non-equilibrium and dispersive flow patterns in both Compiègne sand and gravel media.

The hydrodynamic parameters with their confidence intervals for all porous media were obtained from HYDRUS simulations, using the physical non-equilibrium model (MIM). A good fitting of the modeled BTCs (Fig. 5a, lines) to the experimental BTCs (Fig. 5a, symbols) with high regression coefficient (R^2>0.98) was obtained for all transport experiments (Table 3). The mean mobile fractions of the total water

volume, θ_m/θ, accessible for convective tracer transport were higher for Fontainebleau sandy columns (96.1%), compared to those obtained for Compiègne sandy (79.4%) and gravel (81.7%) columns (Table 3). The lower θ_m/θ values obtained for both Compiègne sand and gravel implied that in these porous media, a smaller pore water volume than that in the Fontainebleau sand was required for solute transport. These results are in agreement with those obtained by Lamy et al.[65] These authors reported θ_m/θ values of 71.0% for the same heterogeneous gravel. The MIM-derived dispersivity (λ) for chloride was in the same order of magnitude as the grain diameter of porous media (Table 3). Thus, higher dispersivity values were obtained for Compiègne sandy (0.82 cm) and gravel (1.93 cm) media compared to the Fontainebleau sand (0.14 cm). This was expected because the dispersivity increased with the increasing of the physical heterogeneity of the porous media.[66] In accordance to these results, Lamy et al. reported similar dispersivity values of 1.97 cm for the same gravel under saturated conditions.[47] The solute exchange rate (α) was much higher for the gravel compared to both sands (Table 3). However, it is difficult to compare solute exchange rate values obtained in different porous media, as this parameter is highly dependent to the geometry of the pores and pore water velocity. High dispersivity values and asymmetrical shape of tracer BTCs with tailing obtained for both Compiègne sand and gravel columns confirmed non-uniform flow in these media. This may be explained by the existence of mobile water regions with high velocity and immobile water regions that do not permit convective flow. Thus, a part of the water tracer could preferentially fill the pore regions with high velocity and move through these regions quickly, while other part of the tracer may diffuse into the immobile water regions. Because of the concentration gradient, the tracer in immobile water regions could slowly diffuse into the mobile water regions causing the "tailing" shown in the breakthrough curves of tracer for both Compiègne sand and gravel media.

3.5.2 Bacteria flow pathways depend on pore size distribution of the media

In Fontainebleau sandy columns the breakthrough of both bacteria (Fig. 5b, 5c) occurred later compared to the tracer (Fig. 5a). This effect was more pronounced for *Klebsiella* sp. strain. This was related to the physical structure of the porous media. As Fontainebleau sand has a lower median grain diameter (d_{50} = 0.36 mm) and pore size

(of 55 μm) than two other porous media, negligible preferential flow path occurred in this medium, as confirmed by high θ_m/θ values (96.1%) obtained for the tracer. Thus, the bacteria breakthrough only occurred from matrix pores, leading to retardation factors higher than 1 (Table 4) and a delay of bacteria breakthrough compared to the tracer (Fig. 5). The delay of bacteria breakthrough has also been reported by Jiang et al.[67] Comparing transport through coarse and fine sandy column under variably saturated conditions, these authors reported significant delay of *E. coli* breakthrough in fine compared to coarse sandy column. Conversely to the homogenous sand, the BTCs of both bacteria exhibited a more symmetrical shape, compared to tracer BTCs for both Compiègne sand and gravel columns. This indicated low bacteria dispersion. The earlier bacteria breakthrough compared to the water tracer in these media and retardation factors lower than 1 (Table 4), suggested that both bacteria were restricted by the effect of pore size exclusion, and they could hardly diffuse into the immobile water regions which mostly existed in the smallest pores of the porous media. Earlier bacteria breakthrough compared to the tracer, due to the pore size exclusion effect, has also been reported by other authors.[17, 66, 68, 69]

The same physical non-equilibrium model was used to simulate *E. coli* (Fig 5b, lines) and *Klebsiella* sp. (Fig. 5c, lines) BTCs for all porous media. A good fitting of MIM-model to experimental BTCs (with regression coefficients higher than 0.91) permitted to obtain bacteria transport parameters (Table 4).

Lower θ_m/θ values were obtained for both *E. coli* (86.1%) and *Klebsiella* sp. (84.4%) in Fontainebleau sand (Table 4) than that of the tracer (Table 3), indicating that lower pore water volumes were required for bacteria transport, comparing to those of the water tracer. Similar to water tracer, θ_m/θ values decreased in the more heterogeneous Compiègne sand compared to the homogenous Fontainebleau sand for both bacteria (from 86.1% in F columns to 64.2% in C columns for *E. coli* and from 84.4% in F columns to 76.4% in C columns for *Klebsiella* sp.) (Table 4). Similar tendency was obtained for *Klebsiella* sp. transport in the gravel (θ_m/θ values decreased to 71.4% in G columns). However this tendency was not confirmed for *E. coli* transport in the gravel. Quite the same values (84.9%) as for the most homogenous sand (86.1%) were obtained in this medium for *E. coli*.

The MIM-derived dispersivity (λ) values of *E. coli* and *Klebsiella* sp. through Fontainebleau sandy column (Table 4) were in the same order of magnitude as those

of tracer (Table 3). *Klebsiella* sp. presented a lower dispersivity (0.16 cm) compared to *E. coli* (0.49 cm). However, the dispersivity values of both bacteria through Compiègne sandy and gravel columns (Table 4) were smaller than those of tracer (Table 3). This indicated that bacteria accessed a more restricted part of the pore network and followed a different flow path compared to tracer, because of the size exclusion effect. Lower dispersivity of bacteria compared to water tracer has also been reported by Pang et al.[62]

3.5.3 The role of pores size and their distribution on transport processes

3.5.3.1 The role of pores size and their distribution on water flow

Many studies have shown that water flow is strongly affected by grain/pore sizes[23, 32, 34, 70-72] as well as pore size distribution.[18, 33, 35, 73] As it was expected, the more uniform flow, with higher θ_m/θ and lower dispersivity, was observed from tracer experiments for the most homogenous sand, which has a low mean pore diameter (55µm) and a more homogenous pore size distribution compared to the other media (Fig. 2). The increase of the mean pore diameter, from 55 µm for the homogenous sand to 108 µm for the heterogeneous sand, resulted in a decrease of θ_m/θ and an increase of dispersivity values, as it was expected (Fig. 2). The gravel medium revealed a wide range of pore size distribution constituted by three peak shape pore size distribution: a first peak with small pores obtained at 0.035 µm, a second one with larger pores of 15 µm and a third one of 200 µm. This non-uniform pore size distribution resulted in low θ_m/θ and high dispersivity values. However, similar flow pathways, confirmed by similar θ_m/θ and dispersivity values, were obtained for both Compiègne sand and gravel, even though these two media differed in term of pore size distribution. Fig. 2 showed that the pore size distribution of Compiègne sand was similar to that of Fontainebleau sand, and one may expect more similarity in term of flow pathways, if the pore size distribution is the predominant parameter that governs water flow. These results showed that it is hazardous to reach conclusive results, regarding water flow based only on the pore size distribution of the porous media. The coupled effect of the grains/pores size as well as their distribution may affect water flow. θ_m/θ and dispersivity values, which are macroscopic parameters, are obtained for the whole pore volume domain, without making distinction between micropores and macropores. Other research work at the pore scale is needed to refine these results. Other authors highlighted that the connectivity of the pores and their distribution

highly affect water flow.[31, 74] Our θ_m/θ and dispersivity values for the gravel are consistent with literature studies, which reported low mobile water volumes in strongly heterogeneous soils.[62] However, Lamy et al.[47] reported lower θ_m/θ values for the gravel, than those obtained in this work. These variations could be explained by the differences in experimental conditions such as the column length and Darcian velocity, which may greatly influence the water flow partitioning.

3.5.3.2 The role of pores size and their distribution on bacteria transport

Lower retardation factors and early breakthroughs of both *E. coli* and *Klebsiella* sp. were obtained for the heterogeneous Compiègne sand and gravel, comparing to homogenous sand, indicating preferential transport in these media. Similar to this work, grain and/or pore size role on bacteria transport has been investigated by many authors and breakthrough curves of microspheres and bacteria were found to be sensitive to changes in sand grain size.[75] Jiang et al. suggested that particle size significantly influenced *E. coli* transport and retention. *E. coli* recovery in leachate from coarse sand was significantly higher than for fine sand columns.[67]

Under certain experimental conditions, bacteria may plug or alter the flow. Bacteria may be retained in the porous media, reducing the pore space available for water flow. In addition, bacteria growth during transport experiments may cause biofilm formation, which in turn may modify the permeability. However, under the current experimental conditions of this work bacteria did not plug or alter the flow. The overall mass balances lower than 100% (Table 4) for each bacterium indicated no bacteria growth during transport experiments.

Similar to tracer results, the increase of the pore size and total porosity of sandy media with similar pore size distributions resulted in a decrease of θ_m/θ values for *Klebsiella* sp., causing non-uniform transport in the most heterogeneous sand, in accordance with literature studies (Fig. 6). The increase of the total porosity of porous media resulted in a decrease of θ_m/θ values for this strain, enhancing preferential transport (low θ_m/θ) in the heterogeneous gravel (Fig. 6). *Klebsiella* sp. recovery in the effluent, M_{eff}, increased with increasing preferential transport, θ_m/θ, and porosity of the porous media. These results indicated that *Klebsiella* sp. collected at the column outlet travel through larger interconnected pores with high pore velocity and is excluded from a portion of the total porosity related to the smallest pores. Similar to

these results, Bradford et al. who reported that grain and pore size distribution were positively correlated, and the presence of larger pores resulted in enhanced colloid transport.[76]

Preferential *E. coli* transport increased from homogenous (F) sand to heterogeneous one (C) with higher porosity, but this non-uniform transport did not result in an increase of the *E. coli* mass recovery in the effluent, contrary to what has been observed for *Klebsiella* sp. in the same sands (Fig. 6). Indeed, no linear relationship between non-uniform transport, porosity and mass recovery in the effluent was obtained for this strain. Similar *E. coli* pathways, confirmed by similar θ_m/θ values, were obtained for both the most homogenous sand and the gravel, even though these two media differed in term of pore sizes as well as pore size distribution and total porosity. In addition, similar *E. coli* recovery was obtained in the effluent for all porous media, contrary to literature results of Bradford et al.[76] and to *Klebsiella* sp. in this study.

The differences obtained between the two bacteria indicated that under these experimental conditions the pore size distribution is not the predominant factor to explain the differences in transport parameters. It should be noted that *E. coli* is a motile strain, while *Klebsiella* sp. is a non-motile one. This characteristic should be involved in bacteria transport behavior in porous media. The results obtained by de Kerchove and Elimelech showed that the ability of the cell to swim is an important factor that enhances the transport. They hypothesized that cell motility allows the upstream swimming of bacteria and subsequent cell deposition on regions which are otherwise inaccessible to non-motile cell deposition.[43] The diffusion coefficient for motile bacteria has been reported to be up to three orders of magnitude greater than non-motile bacteria.[77] This may explain the lower mass recovery of the motile E. coli in the heterogeneous gravel, compared to the non-motile *Klebsiella* sp. The small pores of this medium may not be accessible for the non-motile bacteria, but the motile *E. coli* may have access due to its swimming motility. This may increase the possibility to be trapped in these regions, causing low recovery in the effluent.

3.5.3.3 The role of pores size and their distribution on bacteria retention

Mass percentage of cells recovered from effluent (M_{eff}) was calculated from the analysis of the zero- and first- order moments of the bacterial breakthrough curves

for each porous media and mass percentage of cells retained in the column ($M_{retained}$) was obtained by CFU counts after transport experiments (Table 4). A good total mass balance (M_{total}) of the bacteria recovered in the effluent and retained in the porous media was obtained for all transport experiments.

Both bacteria exhibited a different behavior in term of retention in the porous materials. Similar mean retention ($M_{retained}$) was obtained for *E. coli* in all porous media (Table 4), indicating no influence of the pore size distribution in the retention under the experimental conditions of this work. Conversely, non-motile *Klebsiella* sp. retention was highly dependent on the pore size distribution of the porous media (Table 4). The mean retention of *Klebsiella* sp. decreased with the increasing degree of porous media heterogeneity: higher retention was obtained in the Fontainebleau sand (39.4%) compared to 35.8% in Compiègne sand and 6.5% in gravel, presenting a wide range of the pore size distribution (Fig.2). Similar conclusion was obtained by Bradford et al. who reported that grain and pore size distribution were positively correlated, and the presence of larger pores resulted in enhanced colloid transport.[76] However this tendency was not confirmed for motile *E. coli*.

Results similar to experimental observations were obtained from numerical simulations. Similar MIM-fitted k_{att} values with the same order of magnitude were obtained for *E. coli* in all porous media (Table 4). For each porous media, the MIM-fitted k_{att} value of *E. coli* was larger than that of *Klebsiella* sp. (Table 3), suggesting that there was greater attachment of *E. coli* than *Klebsiella* sp.. The motility of cells may impact the retention behavior. Thus, higher collisions of *E. coli* cells to the grains surface than for *Klebsiella* sp. may be expected due to its motility. This may effectively enhance *E. coli* "diffusion", thereby resulting in a higher attachment of this strain. The DLVO calculations (Table 2) also confirmed these findings. Repulsive electrostatic interactions with the three porous media were greater for *Klebsiella* sp. compared to *E. coli*, which should greatly reduce the potential of *Klebsiella* sp. to be retained. This was also in accordance with the observations of Becker et al. who reported greater attachment rate for motile bacteria in comparison with their non-motile mutants in the coated and clean beads column study.[42]

Other studies suggested a relationship between flow uniformity and colloid retention in porous media. Thus, Lamy et al.[47] found that the increasing of flow uniformity promote colloid retention (latex particles of 1 μm diameter). A more

uniform flow means more pores accessible to the flow and thus more surface of contact between the colloids and the matrix. The improvement of such contact means a higher possibility of colloid entrapment. Conversely, non-uniform or preferential flow pathways disfavor colloid retention. In this work lower retention was obtained for the non-motile *Klebsiella* sp. in porous media exhibiting more preferential flow pathways (i.e. gravel), results which are in accordance to what has been reported in the literature for colloids. However contradictory results were obtained for the motile *E. coli*. Similar retention values were obtained for *E. coli* for all porous media, indicating no obvious relationship between flow uniformity and motile bacteria retention.

4. Conclusion

Conservative tracer and bacteria transport experiments were carried out in porous media with distinct pore size distribution under steady state and saturated flow conditions. The results obtained from both experimental observations and numerical simulations indicated that:

- Water flow was highly dependent to the physical heterogeneity of the porous media. More non-uniform and dispersive flow patterns occurred in both heterogeneous sand and gravel media compared to those of the homogenous sand. However, similar flow pathways obtained for both heterogeneous sand and gravel, even though these two media differed in term of pore size distribution, showed that it is hazardous to reach conclusive results, regarding water flow based only on the pore size distribution of the porous media. Other factor like the connectivity of the pores should be investigated to provide a better characterization of water flow processes.

- Bacteria flow pathways differed from water flow pathways. Bacteria transport occurred through more preferential flow pathways compared to the water tracer. The preferential *Klebsiella* sp. transport increased with the increasing of the physical porous media heterogeneity. Higher amount of bacteria mass recovery in the effluent with increasing preferential transport indicated that *Klebsiella* sp. transport occurred through larger interconnected pores with high pore velocity and was excluded from a portion of the total porosity related to the smallest pores. Preferential transport reduced non-motile *Klebsiella* sp. retention in the porous medium, by reducing the contact between bacteria and retention sites. But this trend was not confirmed for the motile *E. coli*. No linear relationship between non-uniform transport,

porosity, mass recovery in the effluent, and retention was obtained for this strain. These differences in bacteria behavior should be linked to bacteria characteristics, like motility, which greatly affect transport properties that even big differences in the physical heterogeneity of the porous media may not compensate.

Acknowledgments

This work was financially supported by research funds from Université de Technologie de Compiègne and China Scholarship Council.

References

1. G. Gargiulo, S. A. Bradford, J. Šimůnek, P. Ustohal, H. Vereecken and E. Klumpp, *J. Contam. Hydrol.* , 2007, **92**, 255-273.
2. Y. Jin, Y.J. Chu and Y. S. Li, *J. Contam. Hydrol.* , 2000, **43**, 111-128.
3. T. R. Ginn, B. D. Wood, K. E. Nelson, T. D. Scheibe, E. M. Murphy and T. P. Clement, *Adv. Water Resour.*, 2002, **25**, 1017-1042.
4. K. A. Reynolds, *Water Condit. Purif.* , 2004, **56**, 28-30.
5. T. K. Sen, D. Das, K. C. Khilar and G. K. Suraishkumar, *Colloids Surf. A: Physicochem. Eng. Aspects*, 2005, **260**, 53-62.
6. D. L. Craig, H. J. Fallowfield and N. J. Cromar, *J. Appl. Microbiol.*, 2002, **93**, 557-565.
7. A. D. Ferguson and J. Deisenhofer, *Cell*, 2004, **116**, 15-24.
8. K. J. Indest, K. Betts, J. S. Furey, H. L. Fredrickson and V. R. Hinton, *Aquat. Ecosyst. Health Manage.* , 2004, **7**, 415-424.
9. A. I. Zouboulis, M. X. Loukidou and K. A. Matis, *Process Biochem.*, 2004, **39**, 909-916.
10. C. Ferguson, A. M. de Roda Husman, N. Altavilla, D. Deere and N. Ashbolt, *Environ. Sci. Technol.* , 2003, **33**, 299-361.
11. A. A. Keller and A. Maria, *Adv. Water Resour.*, 2007, **30**, 1392-1407.
12. A. B. Cunningham, R. R. Sharp, F. Caccavo and R. Gerlach, *Adv. Water Resour.*, 2007, **30**, 1583-1592.
13. N. Tufenkji, J. N. Ryan and M. Elimelech, *Environ. Sci. Technol.* , 2002, **36**, 422a-428a.
14. N. Tufenkji, G. F. Miller, J. N. Ryan, R. W. Harvey and M. Elimelech, *Environ. Sci. Technol.* , 2004, **38**, 5932-5938.

15. G. Chen and K. A. Strevett, *Environ. Microbiol.*, 2001, **3**, 237-245.
16. G. Lutterodt, M. Basnet, J. W. A. Foppen and S. Uhlenbrook, *Water Res.*, 2009, **43**, 595-604.
17. A. Safadoust, A. A. Mahboubi, M. R. Mosaddeghi, B. Gharabaghi, A. Unc, P. Voroney and A. Heydari, *J. Hydrol.*, 2012, **430-431**, 80-90.
18. J. W. A. Foppen, A. Mporokoso and J. F. Schijven, *J. Contam. Hydrol.*, 2005, **76**, 191-210.
19. M. J. Hendry, J. R. Lawrence and P. Maloszewski, *Ground Water*, 1999, **37**, 103-112.
20. C. H. Bolster, A. L. Mills, G. M. Hornberger and J. S. Herman, *J. Contam. Hydrol.*, 2001, **50**, 287-305.
21. N. Sepehrnia, A. A. Mahboubi, M. R. Mosaddeghi, A. A. Safari Sinejani and G. Khodakaramian, *Geoderma*, 2014, **217-218**, 83-89.
22. A. A. Keller, S. Sirivithayapakorn and C. V. Chrysikopoulos, *Water Res. Resour.*, 2004, **40**, doi: 10.1029/2003WR002676.
23. V. I. Syngouna and C. V. Chrysikopoulos, *J. Contam. Hydrol.*, 2011, **126**, 301-314.
24. S. A. Bradford, J. Šimůnek and S. L. Walker, *Water Resour. Res.* , 2006, **42**, W12S12, doi:10.1029/2005WR004805.
25. J. W. A. Foppen and J. F. Schijven, *Water Res.*, 2005, **39**, 3082-3088.
26. R. Anders and C. V. Chrysikopoulos, *Transport Porous Med.*, 2009, **76**, 121-138.
27. F. D. Castro and N. Tufenkji, *Environ. Sci. Technol.* , 2007, **41**, 4332-4338.
28. S. B. Kim, S. J. Park, C. G. Lee, N. C. Choi and D. J. Kim, *Colloids Surf. B: Biointerfaces* 2008, **63**, 236-242.
29. G. Sadeghi, J. F. Schijven, T. Behrends, S. M. Hassanizadeh, J. Gerritse and P. J. Kleingeld, *Ground Water* 2011, **49**, 12-19.
30. H. B. Zhang, N. A. Nordin and M. S. Olson, *J. Contam. Hydrol.*, 2013, **150**, 54-64.
31. Y. S. Wang, S. A. Bradford and J. Šimůnek, *J. Contam. Hydrol.* , 2014, **159**, 57-66.
32. C. Shani, N. Weisbrod and A. Yakirevich, *Colloids Surf. A: Physicochem. Eng. Aspects*, 2008, **316**, 142-150.
33. A. Benamar, N. D. Ahfir, H. Q. Wang and A. Alem, *C. R. Geoscience*, 2007,

339, 674-681.

34. Y. Y. Sun, B. Gao, S. A. Bradford, L. Wu, H. Chen, X. Q. Shi and J. C. Wu, *Water Res.*, 2015, **68**, 24-33.

35. B. B. Ding, C. L. Li, M. Zhang, F. Ji and X. Q. Dong, *Chem. Eng. Sci.*, 2015, http://dx.doi.org/10.1016/j.ces.2015.1001.1012.

36. D. E. Fontes, A. L. Mills, G. M. Hornberger and J. S. Herman, *Appl. Environ. Microbiol.* , 1991, **57**, 2473-2481.

37. B. Gharabaghi, A. Safadoust, A. A. Mahboubi, M. R. Mosaddeghi, A. Unc, B. Ahrens and G. Sayyad, *J. Hydrol.*, 2015, **522**, 418-427.

38. F. K. Leij and S. A. Bradford, *J. Contam. Hydrol.*, 2013, **150**, 65-76.

39. K. F. Fong and A. L. Mulkey, *Water Resour. Res.*, 1990, **26**, 1291-1303.

40. H. H. Gerke and M. T. Van Genuchten, *Water Resour. Res.*, 1993, **29**, 305-319.

41. M. L. Brusseau, Z. Gerstl, D. Augustijn and P. S. C. Rao, *J. Hydrol.* , 1994, **163**, 187-193.

42. M. W. Becker, S. A. Collins, D. W. Metge, R. W. Harvey and A. M. Shapiro, *J. Contam. Hydrol.*, 2004, **69**, 195-213.

43. A. J. de Kerchove and M. Elimelech, *Environ. Sci. Technol.*, 2008, **42**, 4371-4377.

44. S. L. Walker, J. A. Redman and M. Elimelech, *Environ. Sci. Technol.*, 2005, **39**, 6405-6411.

45. G. Gargiulo, S. A. Bradford, J. Šimůnek, P. Ustohal, H. Vereecken and E. Klumpp, *Vadose Zone J.*, 2008, **7**, 406-419.

46. C. H. Bolster, S. L. Walker and K. L. Cook, *J. Environ. Qual.* , 2006, **35**, 1018-1025.

47. E. Lamy, L. Lassabatere, B. Bechet and H. Andrieu, *Geotext. Geomenbranes*, 2013, **36**, 55-65.

48. E. Tait, S. P. Stanforth, S. Reed, J. D. Perry and J. R. Dean, *RSC Adv.*, 2015, **5**, 15494-15499.

49. R. Podschun, S. Pietsch, C. Höller and U. Ullmann, *Appl. Environ. Microbiol.*, 2001, **67**, 3325-3327.

50. R. Sharmeen, M. N. Hossain, M. M. Rahman, M. J. Foysal and M. F. Miah, *Int. Curr. Pharma. J.* , 2012, **1**, 133-137.

51. K. Sankaran, L. Pisharody, G. S. Narayanan and M. Premalatha, *RSC Adv.*, 2015, **5**, 70977-70984.

52. A. L. Mills, C. Breuil and R. R. Colwell, *Can. J. Microbiol.*, 1978, **24**, 552-557.
53. D. G. Brown, J. R. Stencel and P. R. Jaffé, *Water Res.* , 2002, **36**, 105-114.
54. M. B. Salerno, M. Flamm, B. E. Logan and D. Velegol, *Environ. Sci. Technol.*, 2006, **40**, 6336-6340.
55. S. Xu, Q. Liao and J. E. Saiers, *Environ. Sci. Technol.* , 2008, **42**, 771-778.
56. T. Schinner, A. Letzner, S. Liedtke, F. D. Castro, I. A. Eydelnant and N. Tufenkji, *Water Res.*, 2010, **44**, 1182-1192.
57. J. A. Redman, S. L. Walker and M. Elimelech, *Environ. Sci. Technol.*, 2004, **38**, 1777-1785.
58. G. Qiao, H. Li, D. H. Xu and S. Park, *J. Bacteriol. Parasitol.*, 2012, **3**, 1-6.
59. M. A. Ascon-Cabrera and J. M. Lebeault, *J. Ferment. Bioeng.*, 1995, **80**, 270-275.
60. M. Sardin, D. Schweich, F. J. Leij and M. T. van Genuchten, *Water Res. Resour.* , 1991, **27**, 2287-2307.
61. M. T. van Genuchten and P. J. Wieranga, *Soil Sci. Soc. Am. J.*, 1976, **40**, 473-480.
62. L. P. Pang, M. McLeod, J. Aislabie, J. Šimůnek, M. Close and R. Hector, *Vadose Zone J.*, 2008, **7**, 97-111.
63. E. M. V. Hoek and G. K. Agarwal, *J. Colloid Interface Sci.*, 2006, **298**, 50-58.
64. M. W. Hahn and C. R. O'Mella, *Environ. Sci. Technol.*, 2004, **38**, 210-220.
65. E. Lamy, L. Lassabatere and B. Béchet, *In: Proceeding of the 11th International Conference on Urban Drainage Edinburgh*, 2008, Scotland, UK.
66. J. Levy, K. Sun, R. H. Findlay, F. T. Farruggia, J. Porter, K. L. Mumy, J. Tomaras and A. Tomaras, *J. Contam. Hydrol.* , 2007, **89**, 71-106.
67. G. M. Jiang, M. J. Noonan, G. D. Buchan and N. Smith, *J. Contam. Hydrol.*, 2007, **93**, 2-20.
68. G. M. Jiang, M. J. Noonan, D. B. Graeme and S. Neil, *Aust. J. Soil Res.*, 2005, **43**, 695-703.
69. A. Safadoust, A. A. Mahboubi, M. R. Mosaddeghi, B. Gharabaghi, P. Voroney, A. Unc and G. Khodakaramian, *J. Environ. Manage.* , 2012, **107**, 147-158.
70. C. V. Chrysikopoulos and A. F. Aravantinou, *J. Environ. Chem. Eng.*, 2014, **2**, 796-801.
71. D. Kasel, S. A. Bradford, J. Šimůnek, M. Heggen, H. Vereecken and E.

Klumpp, *Water Res.*, 2013, **47**, 933-944.

72. P. N. Mitropoulou, V. I. Syngouna and C. V. Chrysikopoulos, *Chem. Eng. J.*, 2013, **232**, 237-248.

73. D. Prédélus, L. Lassabatere, A. P. Coutinho, C. Louis, T. Brichat, E. B. Slimène, T. Winiarski and R. Angulo-Jaramillo, *J. Water Resource Prot.*, 2014, **6**, 696-709.

74. E. Lamy, L. Lassabatere, B. Bechet and H. Andrieu, *J. Hydrol.*, 2009, **376**, 392-402.

75. P. S. K. Knappett, M. B. Emelko, J. Zhang and L. D. McKay, *Water Res.*, 2008, **42**, 4368-4378.

76. S. A. Bradford, S. R. Yates, M. Bettahar and J. Šimůnek, *Water Resour. Res.*, 2002, **38**, 1327, doi: 1310.1029/2002WR001340.

77. T. A. Camesano and B. E. Logan, *Environ. Sci. Technol.*, 1998, **32**, 1699-1708.

Table 1. Experimental conditions for all tracer and bacteria experiments.

Tracer/ Bacteria	Replicate	Initial concentration[a]	Porosity (%)	Bulk density (g/cm^3)	Pulse time (min)	Darcy velocity (cm/min)
			Fontainebleau sandy column			
	Exp.1		34.5	1.74	5.48	0.439
	Exp.2		34.2	1.74	5.48	0.436
	Exp.3	0.01	33.8	1.75	5.43	0.442
	Average		34.2 (0.35)[b]	1.74 (0.01)	5.46 (0.03)	0.439 (0.003)
			Compiègne sandy column			
	Exp.1		45.2	1.46	5.63	0.428
	Exp.2		43.9	1.50	5.67	0.427
Tracer	Exp.3	0.01	44.0	1.50	5.67	0.424
	Average		44.4 (0.723)	1.49 (0.023)	5.66 (0.023)	0.426 (0.002)
			The gravel column			
	Exp.1		79.0	0.52	5.65	0.419
	Exp.2		78.1	0.55	5.68	0.413
	Exp.3	0.05	78.5	0.53	5.58	0.428
	Average		78.5 (0.451)	0.53 (0.015)	5.64 (0.051)	0.420 (0.008)
			Fontainebleau sandy column			
	Exp.1	9.08×10^8	35.0	1.72	5.55	0.416
	Exp.2	5.62×10^8	34.3	1.74	5.62	0.423
	Exp.3	6.29×10^8	34.4	1.74	5.55	0.426
	Average	6.99×10^8 (1.84×10^8)	34.6 (0.379)	1.73 (0.012)	5.57 (0.040)	0.422 (0.005)
			Compiègne sandy column			
	Exp.1	9.20×10^8	44.2	1.49	5.55	0.418
	Exp.2	7.08×10^8	44.7	1.48	5.50	0.429
E.coli	Exp.3	8.40×10^8	44.8	1.47	5.47	0.431
	Average	8.23×10^8 (1.07×10^8)	44.6 (0.321)	1.48 (0.01)	5.51 (0.040)	0.426 (0.007)
			The gravel column			
	Exp.1	5.60×10^8	77.6	0.56	5.68	0.421
	Exp.2	6.52×10^8	77.7	0.56	5.50	0.423
	Exp.3	5.30×10^8	77.2	0.57	5.67	0.424
	Average	5.81×10^8 (0.64×10^8)	77.5 (0.265)	0.56 (0.006)	5.62 (0.101)	0.423 (0.002)
			Fontainebleau sandy column			
	Exp.1	5.58×10^8	34.7	1.73	5.68	0.415
Klebsiella sp.	Exp.2	4.84×10^8	33.3	1.77	5.67	0.416
	Exp.3	5.98×10^8	33.8	1.75	5.68	0.416
	Average	5.47×10^8	33.9	1.75	5.68	0.416

	(0.58×10^8)	(0.709)	(0.02)	(0.006)	(0.0006)
		Compiègne sandy column			
Exp.1	6.36×10^8	45.2	1.46	5.63	0.425
Exp.2	4.08×10^8	43.9	1.50	5.55	0.424
Exp.3	4.52×10^8	44.0	1.50	5.60	0.423
Average	4.99×10^8 (1.21×10^8)	44.4 (0.723)	1.49 (0.023)	5.59 (0.040)	0.424 (0.001)
		The gravel column			
Exp.1	5.59×10^8	79.0	0.52	5.68	0.418
Exp.2	6.00×10^8	78.1	0.55	5.68	0.414
Exp.3	6.70×10^8	78.5	0.53	5.50	0.428
Average	6.10×10^8 (0.56×10^8)	78.5 (0.451)	0.53 (0.015)	5.62 (0.104)	0.420 (0.007)

[a] Tracer concentration is given in mol/L and bacteria concentration in CFU/mL.

[b] The values given in parentheses are the standard deviations of triplicate columns.

Table 2. Bacteria and porous media Zeta potentials, as well as the calculated DLVO parameters.

Zeta potential (mV)		Energy barrier (kT)	Secondary minimum depth (kT)	Secondary minimum separation (nm)
Bacteria	Porous media			
-41.1 ± 0.65 (*E. coli*)	-39.6 ± 1.8 (F)	1586	0.40	300
	-20.5 ± 1.8 (C)	814	0.49	287
	-12.5 ± 1.8 (G)	43.5	2.8	27
-33.2 ± 0.29 (*Klebsiella* sp.)	-39.6 ± 1.8 (F)	1778	0.58	309
	-20.5 ± 1.8 (C)	909	0.63	311
	-12.5 ± 1.8 (G)	40.2	4.6	28

Table 3. Solute transport parameters: mass balance (*MB*) and retardation factors obtained from experimental observations, and fitted HYDRUS-1D transport parameters for triplicate columns (dispersivity λ, mobile fraction θ_m/θ, and solute exchange rate α).

Replicate	*MB* (%)	Retardation factor	λ (cm)		θ_m/θ (%)		α (min^{-1})		R^2
			Value	S.E.Coeff.[b]	Value	S.E.Coeff.	Value	S.E.Coeff.	
Fontainebleau sandy column									
Exp.1	99.4	0.98	0.19	9.86E-03	94.8	7.54E-04	1.03E-04	3.38E-04	0.996
Exp.2	99.4	1.01	0.11	1.68E-03	97.3	1.23E-03	1.91E-04	3.51E-04	0.999
Exp.3	99.2	1.01	0.11	2.86E-03	96.1	3.52E-04	4.83E-04	1.31E-04	0.999
Average	99.3 (0.12)[a]	1.00 (0.02)	0.14 (0.05)		96.1 (1.25)		2.59E-04 (1.99E-04)		0.998 (0.002)
Compiègne sandy column									
Exp.1	97.7	1.06	0.80	9.00E-02	77.6	8.45E-04	5.19E-02	1.01E-02	0.985
Exp.2	99.2	1.05	0.84	6.13E-02	81.7	5.89E-03	1.93E-02	2.08E-03	0.991
Exp.3	98.3	1.07	0.80	4.53E-02	78.7	5.91E-04	3.45E-02	3.01E-03	0.990
Average	98.4 (0.75)	1.06 (0.01)	0.82 (0.02)		79.4 (0.02)		3.53E-02 (1.6E-02)		0.989 (0.003)
The gravel column									
Exp.1	100	0.97	1.95	1.33E-01	81.5	2.59E-02	3.40E-01	6.53E-02	0.993
Exp.2	99.7	0.99	1.84	1.89E-01	79.6	2.30E-02	4.60E-01	1.00E+00	0.990
Exp.3	100	1.19	2.01	1.25E-01	84.1	1.49E-02	8.60E-03	1.33E-03	0.997
Average	99.9 (0.17)	1.05 (0.12)	1.93 (0.083)		81.7 (2.2)		2.69E-01 (2.33E-01)		0.993 (0.004)

[a] The values given in parentheses are standard deviations of triplicate columns.

[b] refers to the standard error coefficient obtained from HYDRUS-1D simulations.

Table 4. Bacterial transport parameters: the effluent (M_{eff}), the retained ($M_{retained}$), the total (M_{total}=$M_{retained}$+M_{eff}) mass percentage recovery and the retardation factors obtained from triplicate column experiments, together with fitted HYDRUS-1D bacteria transport parameters (dispersivity λ, mobile fraction θ_m/θ, solute exchange rate α and bacteria attachment rate coefficient k_{att}).

Replicate	M_{eff}	$M_{retained}$	M_{total}	Retardation factor	λ (cm)		θ_m/θ (%)		α (min^{-1})		$k_{att.}$ (min^{-1})		R^2
					Value	S.E.Coeff.[b]	Value	S.E.Coeff.	Value	S.E.Coeff.	Value	S.E.Coeff.	
Fontainebleau sandy column (for *E.coli* transport)													
Exp.1	46.6	41.1	87.7	1.13	0.52	3.32E-01	88.6	7.44E-02	1.85E-02	4.71E-02	0.105	2.29E-03	0.989
Exp.2	45.2	41.3	86.5	1.17	0.60	2.69E-02	86.3	1.23E-02	1.32E-02	1.61E-03	0.118	1.23E-02	0.989
Exp.3	53.9	36.2	90.1	1.10	0.37	9.64E-02	83.3	1.51E-02	1.46E-02	7.75E-03	0.094	1.10E-03	0.991
Average	48.5 (4.7)[a]	39.5 (2.9)	88.1 (1.8)	1.13 (0.04)	0.49 (0.12)		86.1 (2.7)		2.99E-02 (1.60E-02)		0.107 (0.011)		0.990 (0.001)
Compiègne sandy column (for *E.coli* transport)													
Exp.1	50.6	41.6	92.2	0.66	0.15	2.90E-01	64.2	1.20E-02	1.21E-01	7.24E-02	0.192	1.27E-02	0.972
Exp.2	39.2	49.9	89.1	0.76	0.30	9.37E-02	62.7	4.14E-02	1.46E-01	7.26E-02	0.212	7.90E-03	0.994
Exp.3	41.8	43.1	86.9	0.71	0.72	3.45E-01	65.6	1.66E-02	1.18E-01	1.28E-02	0.224	3.31E-02	0.984
Average	43.8 (6.0)	44.9 (4.4)	89.4 (2.7)	0.71 (0.05)	0.39 (0.30)		64.2 (1.5)		1.28E-01 (1.54E-02)		0.211 (0.016)		0.983 (0.011)
The gravel column (for *E.coli* transport)													
Exp.1	52.4	37.1	89.5	0.48	0.50	5.27E-03	83.3	2.10E-03	1.15E-02	9.78E-04	0.156	1.16E-03	0.996
Exp.2	49.3	37.9	87.2	0.45	0.51	7.90E-02	85.2	1.01E-02	9.71E-03	5.26E-03	0.181	1.83E-03	0.996
Exp.3	43.3	43.6	86.9	0.44	0.57	5.57E-02	86.2	6.43E-03	8.91E-03	3.23E-03	0.230	1.20E-03	0.998
Average	48.3 (4.6)	39.5 (3.5)	87.9 (1.4)	0.46 (0.02)	0.52 (0.04)		84.9 (1.5)		1.24E-02 (5.31E-03)		0.187 (0.041)		0.997 (0.001)
Fontainebleau sandy column (for *Klebsiella* sp. transport)													
Exp.1	60.5	32.0	92.5	1.64	0.236	1.66E-02	83.9	4.55E-03	6.17E-03	2.61E-03	0.043	3.06E-03	0.926

Exp.2	42.5	42.5	85.0	1.46	0.11	7.79E-02	86.1	2.07E-02	4.26E-02	9.81E-03	0.075	1.93E-03	0.905
Exp.3	40.2	43.7	83.9	1.38	0.13	1.34E-02	83.1	1.42E-02	7.56E-02	1.86E-02	0.087	1.97E-03	0.914
Average	47.7 (11.1)	39.4 (6.4)	87.1 (4.7)	1.49 (0.13)	0.16 (0.068)		84.4 (1.6)		4.15E-02 (3.47E-02)		0.068 (0.023)		0.915 (0.010)
Compiègne sandy column (for *Klebsiella* sp. transport)													
Exp.1[c]	70.8	25.5	96.3	0.80	0.74	1.96E-02	79.1	1.46E-03	4.90E-03	3.90E-04	0.068	3.67E-03	0.998
Exp.2	44.1	40.8	84.9	0.78	0.13	3.95E-02	76.1	4.32E-03	1.28E-02	2.25E-03	0.159	9.38E-03	0.956
Exp.3	50.4	41.2	91.6	0.84	0.38	3.36E-02	74.0	3.16E-03	1.03E-02	1.51E-03	0.146	1.51E-03	0.998
Average	55.1 (13.9)	35.8 (9.0)	90.9 (5.7)	0.81 (0.03)	0.42 (0.31)		76.4 (2.5)		9.00E-03 (4.00E-03)		0.124 (0.049)		0.984 (0.024)
The gravel column (for *Klebsiella* sp. transport)													
Exp.1	93.9	4.5	98.4	0.50	0.22	2.04E-02	71.7	1.70E-03	3.78E-02	1.30E-03	0.0076	1.04E-03	0.990
Exp.2	98.0	1.2	99.2	0.46	0.11	1.53E-02	70.1	1.21E-03	4.24E-02	4.30E-03	0.0020	3.50E-04	0.988
Exp.3	83.9	13.7	97.6	0.46	0.42	3.71E-02	72.4	3.89E-03	4.60E-02	2.88E-03	0.0265	1.35E-03	0.992
Average	92.0 (7.3)	6.5 (6.5)	98.4 (0.8)	0.47 (0.02)	0.25 (0.15)		71.4 (1.2)		4.21E-02 (4.11E-03)		0.0121 (0.012)		0.990 (0.002)

[a] The values given in parentheses were standard deviations.

[b] refers to the standard error coefficient obtained from HYDRUS-1D code.

[c] The values are not valid because of the large standard deviations compared with the two other experiments.

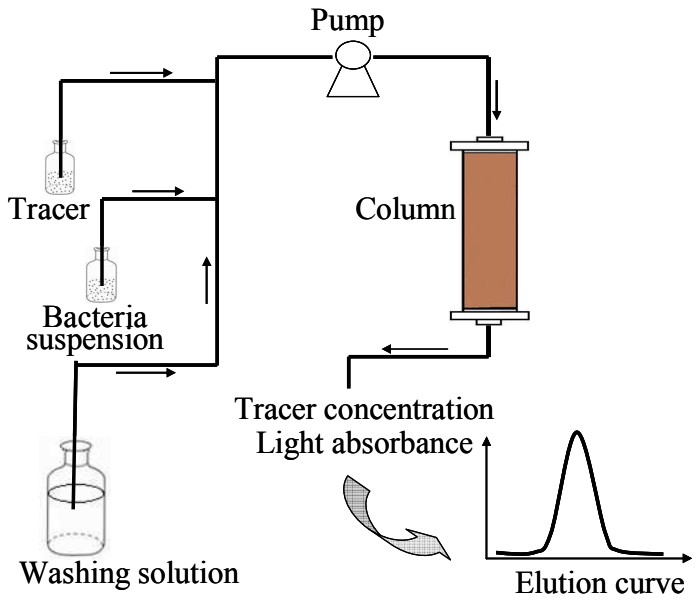

Fig 1. Schematic diagram of transport experimental set-up.

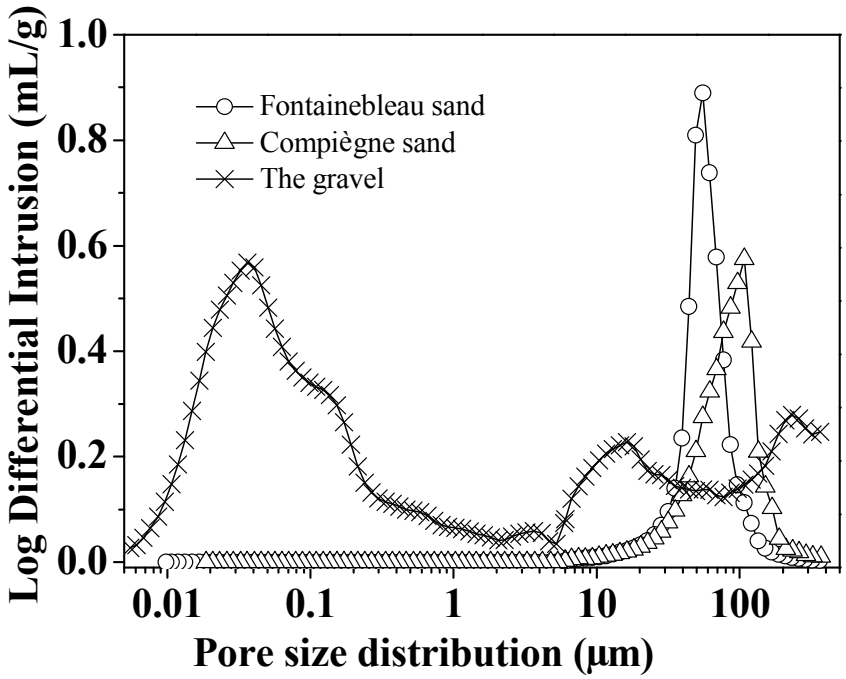

Fig 2. Pore size distribution of the three porous media.

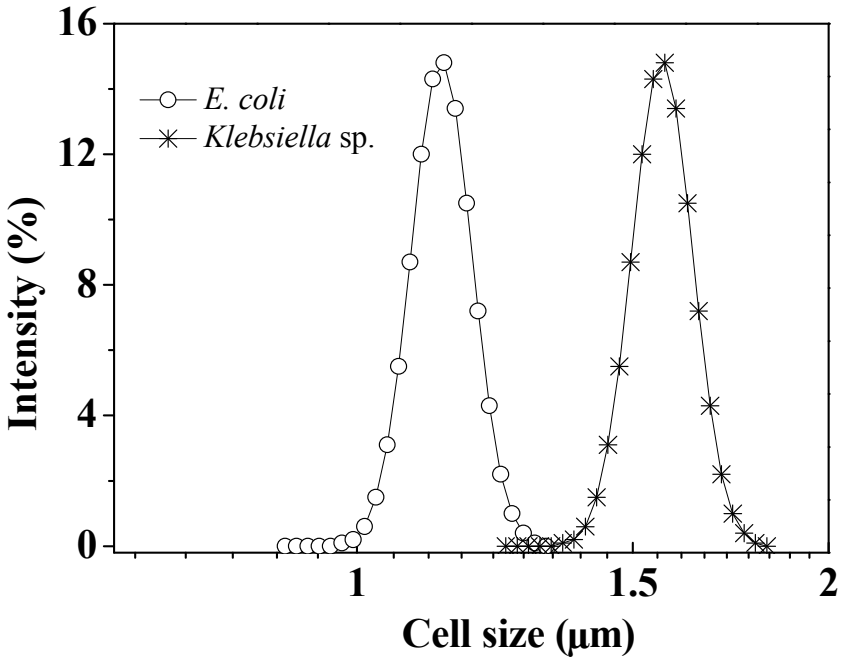

Fig 3. Size distribution of *E. coli* and *Klebsiella* sp. measured in 0.1 mmol/L NaCl solutions.

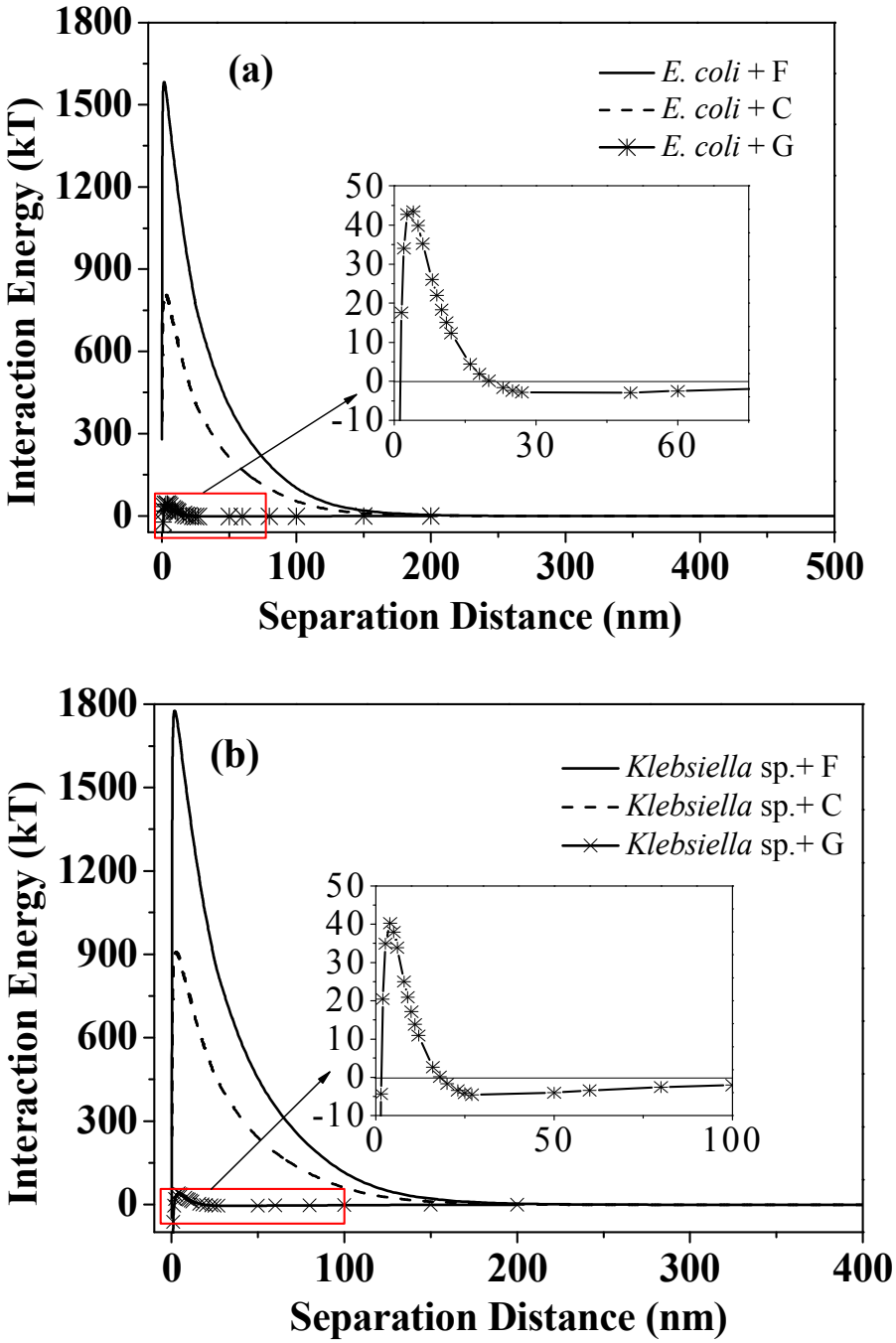

Fig 4. Calculated DLVO energy profiles of interaction between bacteria and porous media.

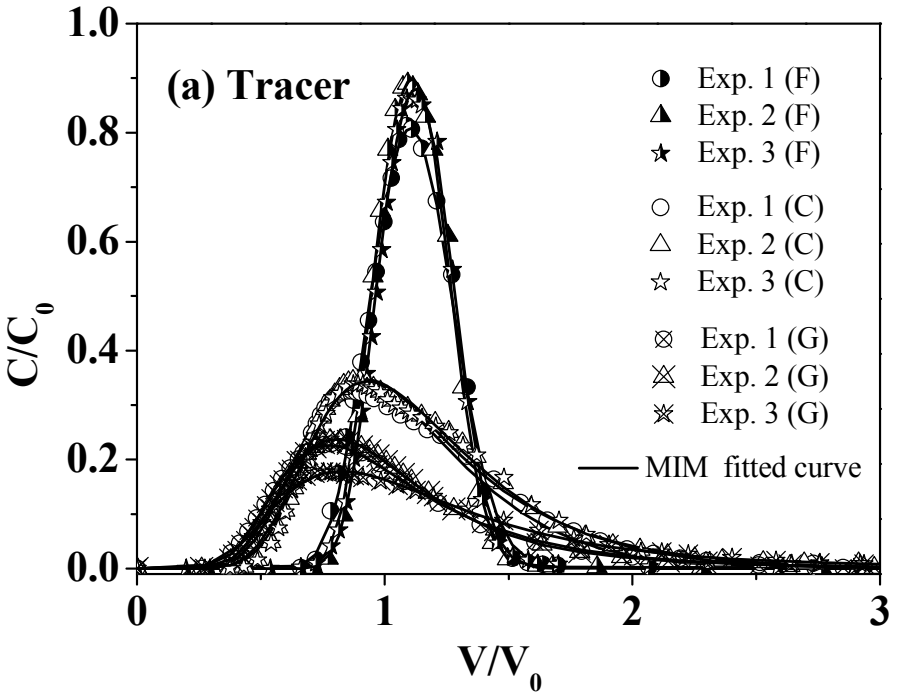

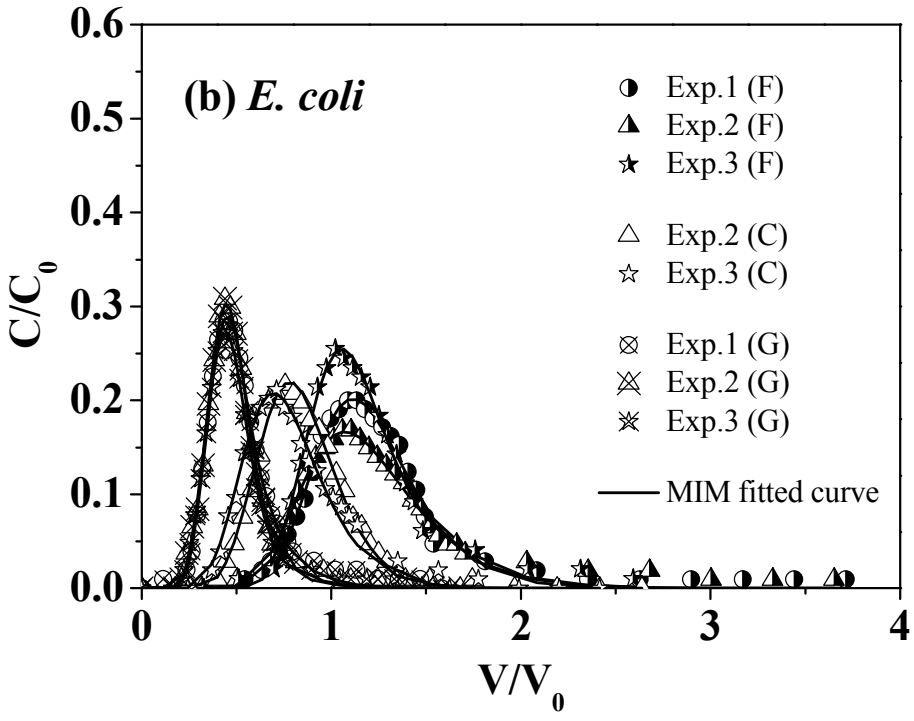

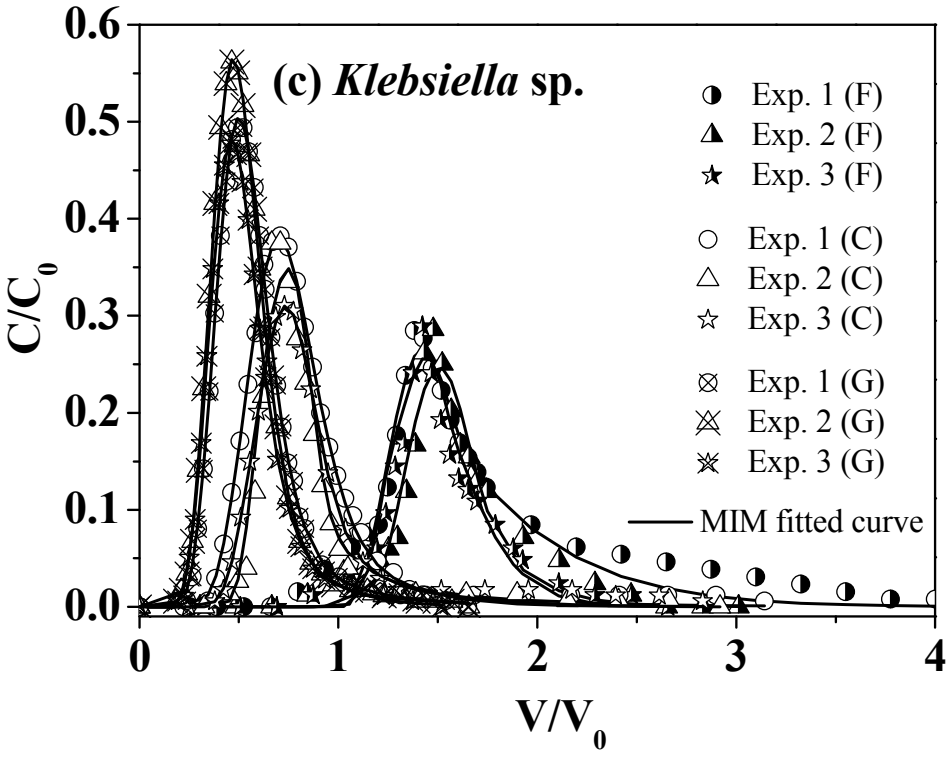

Fig 5. Measured (symbols) and fitted (lines) breakthrough curves of (a) tracer, (b) *E. coli* and (c) *Klebsiella* sp. through three porous media for triplicate columns.

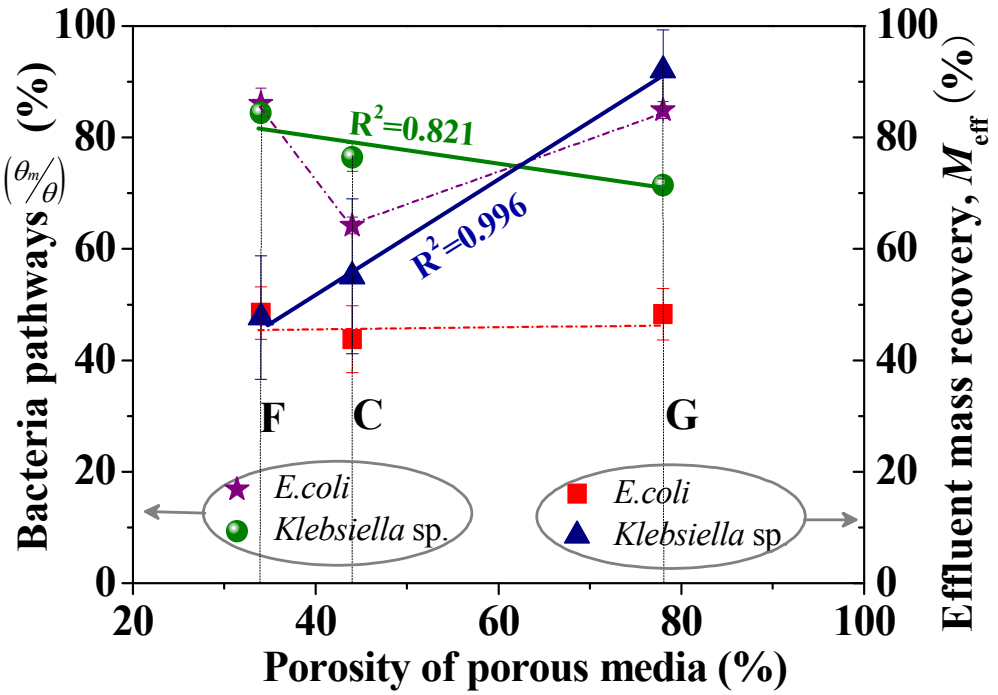

Fig. 6 Relationships between preferential bacteria pathways, bacteria mass recovery from effluent, M_{eff}, and the total porosity of: F – Fontainebleau sand, C – Compiègne sand and G –gravel (mean values with standard deviations of triplicate columns).